Mat. Res. Soc. Symp. Proc. Vol. 692 © 2002 Materials Research Society H9.37

Third Order Mode Optically Pumped Semiconductor Laser for an Integrated Twin Photon Source in Quantum Optics

N. G. Semaltianos, A. De Rossi, V. Berger, B. Vinter, E. Chirlias and V. Ortiz
Thales Research and Technology
Domaine de Corbeville
91404 Orsay, FRANCE

ABSTRACT

Lasing action on a third order waveguide mode is demonstrated at room temperature under optical pumping, in a specifically designed quantum well laser structure. The AlGaAs heterostructure involves barriers which ensure that the third order mode has a higher overlap with the single quantum well emitter than the fundamental mode. Third order mode operation of a laser structure opens the way to modal phase matched parametric down conversion inside the semiconductor laser itself. It is a first step towards the realization of semiconductor twin photon laser sources, needed for quantum information experiments.

INTRODUCTION

Twin photon sources obtained by parametric fluorescence (PF) are a useful tool in quantum cryptography or quantum optics experiments [1-3]. In these experiments PF is obtained from a laser beam with a frequency ω_p which enters into a nonlinear crystal and creates twin down generated photons at a frequency $\omega_i=\omega_s=\omega_p/2$. The whole set-up is in general complicated. The purpose of this work is to study a new type of semiconductor laser in which PF could be obtained in the semiconductor laser itself thus resulting in a highly compact twin photon source.

Two criteria must be fulfilled to obtain efficient PF: a high nonlinear coefficient and the possibility to phase match the interaction between the interacting waves [4]. Semiconductors and especially GaAs are very interesting for waveguided nonlinear parametric processes due to their high nonlinear coefficient and the possibility to integrate quantum well (QW) sources with nonlinear interactions. However, III-V semiconductors are not birefringent and alternative phase matching schemes have to be used [5]. Among the different phase matching schemes, modal dispersion phase matching (MDPM) [6,7] is attractive because it is well suited for materials grown by molecular beam epitaxy (MBE) due to the control of the layer thickness homogeneity up to the atomic level. In this method phase matching is obtained by a careful design of a multilayer waveguide in which the effective indices n_{eff} of three different guided modes i, j and k satisfy the MDPM condition: $n_{eff,i}(\lambda_p)=1/2[n_{eff,j}(\lambda_i)+n_{eff,k}(\lambda_s)]$. Figure 1 indicates MDPM in the laser structure which is described in detail below; in this specific design photons on the third order mode (i=TE_2) at ω_p=775 nm can generate through phase matched PF signal and idler photons at $\lambda_{s,i}=2\lambda_p$=1.55 μm on the fundamental modes (j=TE_0 and k=TM_0). In addition, the overlap integral [6] between the third order mode and the fundamental one, which gives the efficiency of this nonlinear process, is optimised.

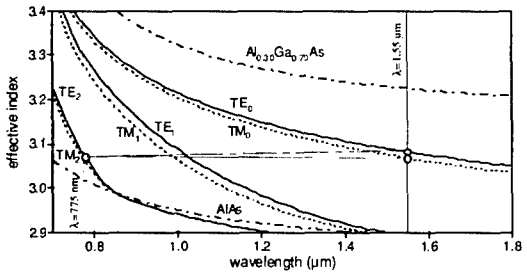

Figure 1. *Effective indices of the sample as a function of wavelength. The two dash-dotted lines show the indices of the $Al_{0.30}Ga_{0.70}As$ (upper curve) and AlAs (lower curve). The triangle joining TE_2 at 775 nm (left open dot) and TE_0 and TM_0 curves at 1.55 μm (two open dots on the right) illustrates the phase matching condition: $n_{TE2}(775nm)=1/2[n_{TE0}(1550nm)+n_{TM0}(1550nm)]$. Note that in this PF scheme, the two down generated photons are cross polarized, which is the best situation for quantum optics applications.*

The purpose of this study is to show that a QW emitter can be used inside this waveguide as a source at ω_p, leading to lasing action on the third order mode, thus well suited for phase matched PF inside the laser cavity. Such a scheme is totally unusual for a semiconductor laser. For this, the electron-hole pairs must recombine in a place where the third order mode has a higher overlap than the two other modes in the system, as explained below.

RESULTS AND DISCUSSION

The sample was grown by a Varian MBE machine, on a semi-insulating GaAs substrate. A 1000 nm AlAs layer (C) was grown followed by a 130 nm $Al_{0.25}Ga_{0.75}As$ generation layer (G); a 140 nm $Al_{0.50}Ga_{0.50}As$ layer (B) and a 100 Å $Al_{0.11}Ga_{0.89}As$ active QW. Then the layers were repeated in the order B/G/C followed finally by a 30nm GaAs cap layer. Figure 2 shows the refractive index profile along the sample depth together with the field distributions of the third order mode (TE_2) and of the fundamental one (TE_0), for a wavelength equal to the expected lasing wavelength (775 nm).

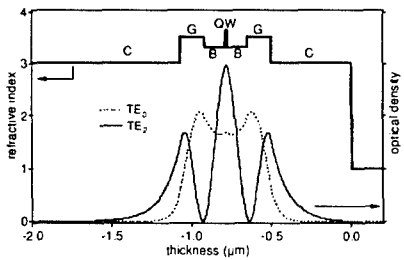

Figure 2. *Refractive index profile with fundamental and third order mode field distributions, for a wavelength of 775 nm, in the TE polarization*

The basic difference between this structure and other laser structures studied so far is the barriers introduced by the two 140 nm $Al_{0.50}Ga_{0.50}As$ B layers. The effect of these barriers is to

enhance the third order mode with respect to the fundamental mode at the QW location, the electric field of the fundamental being reduced in the center of the structure by these two low index layers. As a result, lasing action on the third order mode is expected. However, an additional undesirable effect of the B layers is that they introduce a physical barrier for the difussive exchange of photogenerated carriers between the QW and the G layers, which affects the photoluminescence (PL) efficiency of the QW and of the G layers and may have consequences in the laser power threshold, optical gain and other laser parameters.

The resulting band structure of the sample structure is shown in Figure 3 by taking into account the generation and recombination of electrons and holes in the G layer, their transport to the QW, and their recombination stimulated by the third order mode.

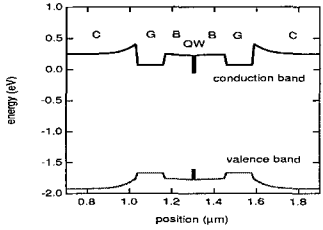

Figure 3. *Band structure of the sample.*

PL spectra from the sample excited by a CW low power (around 5 mW) He:Ne laser at 633 nm (1.958 eV) (Figure 4 (a)), are dominated by two peaks: at 10 K one peak at 1.70 eV related to the excitonic recombination transition between the fundamental state of the conduction band electrons to the fundamental state of the valence band heavy holes of the QW and another one at 1.85 eV related to the band edge excitonic transition from the G layers.

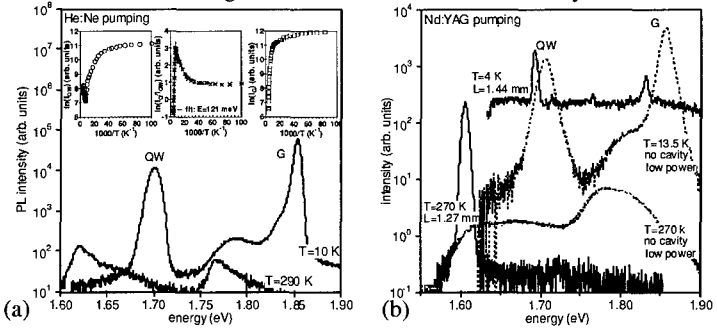

Figure 4. *(a) PL spectra from the sample at low and high temperatures excited by a low power CW He:Ne laser at 633 nm. Inset shows the temperature dependence of the integrated intensities of the peaks related to the QW (I_{QW}), G layers (I_G) and of the ratio (I_G/I_{QW}). In part (b) of the figure a pulsed Nd:YAG laser at 532 nm was used. Dotted line spectra correspond to a low power excitation below threshold, while solid line spectra correspond to transverse pumping of laser bars with cavity lengths L. The lasing peak appears at the low energy side of the spontaneous emission peak.*

In the temperature dependence of the integrated intensities of the two peaks (shown in the insets of Figure 4 (a), it is seen that while the I_G decreases monotonically from low temperatures up to room temperature, the I_{QW} starts increasing above 150 K. This is due to a thermally activated transport of carriers from the G layers to the QW above 150 K with an activation energy of 121 meV estimated from the slope of the straight line behaviour of the ratio of the integrated intensities of the two peaks (I_G/I_{QW}). This energy corresponds to the conduction band offset of the $Al_{0.25}Ga_{0.75}As/Al_{0.50}Ga_{0.50}As$ subsystem (theoretically $\Delta E_{c,G}$=154 meV). By increasing the temperature further above 240 K, I_{QW} starts dropping again. This is due to an increasing importance of thermally activated non-radiative recombination processes at high temperatures, which dominate over the thermal carrier exchange between QW and G layers.

In Figure 4 (b) the sample was pumped by 6 ns pulses from a frequency doubled YAG laser at 532 nm (2.33 eV), at a frequency of 10 Hz. Dotted lines correspond to spontaneous emission spectra with a low excitation power while the solid lines correspond to transverse pumping of cleaved laser bars with cavity length L. Laser emission is observed at 772.5 nm (1.6 eV) at room temperature, near the expected wavelength of 775 nm.

Comparing Figures 4 (a) and (b) it is seen that under He:Ne pumping although at low temperatures I_G is greater than I_{QW}, at room temperature the opposite is true. On the other hand under Nd:YAG pumping I_{QW} is always weaker than I_G even at room temperature, because of the distribution of carrier population in QW and G layers before recombination. However, the inverted population required for stimulated emission is always created first in the QW rather than in the G layers, and this is so in the whole temperature region studied.

The laser power threshold at room temperature was measured equal to 10.7 KW/cm^2 for unprocessed planar samples (as-grown) and 42 KW/cm^2 for processed samples with waveguide ridges (width 10 μm and distance between them around 100 μm). The higher threshold of processed samples as compared to unprocessed ones may be due to the fact that etching of photolithographically made ridges onto the sample surface has as a result oxidation of the AlAs and formation of AlOx [8,9]. The characteristic temperature which expresses the threshold in the exponential empirical form versus sample temperature (Figure 5), was measured equal to 117 K which is comparable to the value reported for III-V lasers in general [10] as well as for ZnSe/ZnSSe blue lasers [11].

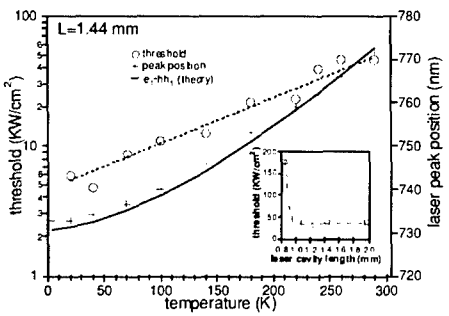

Figure 5. *Laser power threshold and peak position versus temperature. The solid line (through the cross points) corresponds to the theoretically estimated energy of the e_1-hh_1 transition of the QW. Inset shows threshold versus cavity length.*

Both values for the threshold reported above are higher than the value of around 1 KW/cm^2 calculated theoretically from simulations based on Figure3. Apart from stronger recombination in the G layers than simulated, this may be explained by optical losses higher than expected due to optical leakage in the plane of the laser structure, or towards the substrate. Indeed, it can be seen in Figure 1 than the third order mode at 775 nm is near the cut-off of the waveguide (given by the refractive index of the cladding material AlAs), which implies that the mode is very sensitive to scattering processes into leaky waves in the substrate.

Experiments were carried out to measure the far field emission pattern of the semiconductor laser. The signal, shown in Figure 6 as a function of the angle in the transverse direction, starts from a maximum value at 0º, decreases with the angle of rotation to a minimum value at around 20º±3º then obtains a second maximum value at an angle of 40º±3º and finally decreases again to zero.

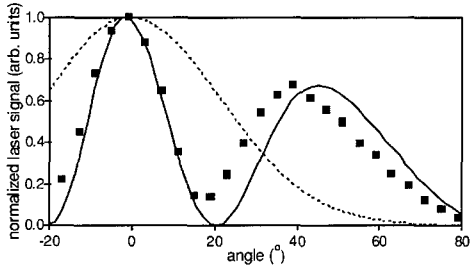

Figure 6. *Laser output signal versus transverse angle of rotation (squares), compared with the calculated far field of third order (full line) and fundamental laser modes (dotted line).*

The solid line in the figure corresponds to theoretical calculation using the Rayleigh-Sommerfeld integral [12] of the far field distribution for a third order mode radiation while the dashed line corresponds to the fundamental mode. As expected, the fundamental mode shows only one main lobe centered at 0º, whereas the third order mode diffraction pattern shows a strong side lobe. Similarity of the experimental points with the theoretical calculated curves for the filed distributions demonstrate that our specially designed laser sample structure emits on the third order mode, as intended.

CONCLUSIONS

We have demonstrated laser emission at 772.5 nm, on a third order waveguide mode, and at room temperature, from an optically pumped AlGaAs QW structure. The structure was characterized in detail in terms of: temperature and pumping energy dependence of photoluminescence spectra and temperature and laser cavity length dependence of power threshold and laser peak position. Further work will include the study of modal phase matching in this semiconductor laser waveguide, in order to provide through intracavity parametric fluorescence a semiconductor source of twin photons.

ACKNOWLEDGEMENTS

This work was performed within the framework of the EC project 'QUCOMM'. N.G.S. is a recipient of a Marie Curie Research Fellowship of the European Community, grant number IST-1999-80034 under the 'QLOPORT' programme.

REFERENCES

1. P. G. Kwiat, K. Mattle, H. Weinfurter, A. Zeilinger, A. V. Sergienko and Y. Shih, *Phys. Rev. Lett.* **75**, 4337 (1995).
2. D. Bouwmeester, J-W. Pan, K. Mattle, M. Eibl, H. Weifurter and A. Zeilinger, *Nature* **390**, 575 (1997).
3. J. W. Pan, D. Bouwmeester, M. Daniell, H. Weinfurter and A. Zeilinger, *Nature* **403**, 515 (2000).
4. A. Yariv, *"Quantum Electronics"* (John Wiley & Sons, New York, 1989).
5. Fiore, V. Berger, E. Rosencher, P. Bravetti and J. Nagle, *Nature* **391**, 463 (1998).
6. M. Jäger, G. I. Stegeman, M. C. Flipse, M. Diemeer and G. Möhlmann, *Appl. Phys. Lett* **69**, 4139 (1996).
7. H. P. Wagner, S. Wittmann, H. Schmitzer and H. Stanzl, *J. Appl. Phys.* **77**, 3637 (1995).
8. J. M. Dallesasse, J. N. Holonyak, Jr., A. R. Sugg, T. A. Richard, *Appl. Phys. Lett.* **57**, 2844 (1990).
9. T. Takamori, K. Takemasa, T. Kamijoh, *Appl. Phys. Lett.* **69**, 659 (1996).
10. H. C. Casey and M. B. Panish, *"Heterostructure Lasers"*, Academic, New York, Ch. 7 (1978).
11. K. Nakanishi, I. Suemune, Y. Fujii, Y. Kuroda and M. Yamanishi, *Appl. Phys. Lett.* **59**, 1401 (1991).
12. M. Born and E. Wolf, *"Principles of Optics"*, (Pergamon Press, Oxford, 1980).